

A Novel Recombinant Vaccinia Virus Expressing the Human Norepinephrine Transporter Retains Oncolytic Potential and Facilitates Deep-Tissue Imaging

Nanhai Chen,¹ Qian Zhang,¹ Yong A Yu,¹ Jochen Stritzker,^{1,2} Peter Brader,^{3,4} Andreas Schirbel,⁵ Samuel Samnick,⁵ Inna Serganova,⁶ Ronald Blasberg,^{3,6} Yuman Fong,⁷ and Aladar A Szalay^{1,2}

¹Genelux Corporation, San Diego Science Center, San Diego, California, United States of America; ²Rudolf Virchow Center for Experimental Biomedicine, Institute for Biochemistry and Institute for Molecular Infection Biology, University of Würzburg, Würzburg, Germany; Departments of ³Radiology, ⁶Neurology and ⁷Surgery, Memorial Sloan-Kettering Cancer Center, New York, New York, United States of America; ⁴Department of Radiology, Division of Pediatric Radiology, Medical University Graz, Austria; ⁵Department of Nuclear Medicine, University of Würzburg, Würzburg, Germany

Noninvasive and repetitive monitoring of a virus in target tissues and/or specific organs of the body is highly desirable for the development of safe and efficient cancer virotherapeutics. We have previously shown that the oncolytic vaccinia virus GLV-1h68 can target and eradicate human tumors in mice and that its therapeutic effects can be monitored by using optical imaging. Here, we report on the development of a derivative of GLV-1h68, a novel recombinant vaccinia virus (VACV) GLV-1h99, which was constructed to carry the human norepinephrine transporter gene (*hNET*) under the VACV synthetic early promoter placed at the *F14.5L* locus for deep-tissue imaging. The hNET protein was expressed at high levels on the membranes of cells infected with this virus. Expression of the hNET protein did not negatively affect virus replication, cytolytic activity in cell culture, or *in vivo* virotherapeutic efficacy. GLV-1h99-mediated expression of the hNET protein in infected cells resulted in specific uptake of the radiotracer (¹³¹I)-meta-iodobenzylguanidine (MIBG). In mice, GLV-1h99-infected tumors were readily imaged by (¹²⁴I)-MIBG positron emission tomography. To our knowledge, GLV-1h99 is the first oncolytic virus expressing the hNET protein that can efficiently eliminate tumors and simultaneously allow deep-tissue imaging of infected tumors.

© 2009 The Feinstein Institute for Medical Research, www.feinsteininstitute.org

Online address: <http://www.molmed.org>

doi: 10.2119/molmed.2009.00014

INTRODUCTION

Oncolytic viral therapy exploits the lifecycle of viruses to specifically infect, replicate within, and lyse cancer cells. Many virus types, including adenoviruses (1), herpes simplex viruses (2), Newcastle disease virus (3), myxoma virus (4), vaccinia virus (VACV) (5), and vesicular stomatitis virus (6), are being investigated as potential agents for oncolytic virotherapy of cancer in

humans. One of the most attractive reasons for using these live vectors is that they generally kill cancer cells that are high in ribonucleotide reductase, high in DNA-repair enzymes, and resistant to apoptosis—all characteristics that would make the tumor cells resistant to chemotherapy and radiation therapy (7,8). VACV is particularly attractive as an agent for human treatment because versions of this virus have been given

to millions of humans during the smallpox eradication campaign (9).

It is of general interest to try to develop imaging techniques that enable tracking of therapeutic gene delivery in gene-therapy protocols. The potential importance of noninvasive tracking techniques in human oncolytic virotherapy trials is well documented. A deep-tissue imaging technique in tracking virus-infected cells in the body may also allow real-time, ongoing assessment of therapy and obviate the need for multiple and repeated tissue biopsies. The tracking of viral delivery could give clinicians the ability to correlate efficacy and therapy, as well as to monitor virus toxicity.

We report the construction and functional testing of an engineered virus strain designed to be traceable by molecular imaging in infected tissues. The cho-

Address correspondence and reprint requests to Aladar A. Szalay, Genelux Corporation, San Diego Science Center, 3030 Bunker Hill Street, Suite 310, San Diego, CA 92109. Phone: 1.858.483.0024; Fax: 1.858.483.0026; E-mail: aaszalay@genelux.com; or Yuman Fong, Department of Surgery, Memorial Sloan-Kettering Cancer Center, 1275 York Avenue, H-1205, New York, NY 10065. Phone: 1.212.639.2016; Fax: 1.646.422.2358; E-mail: fongy@mskcc.org. Submitted February 20, 2009; Accepted for publication February 24, 2009; Epub (www.molmed.org) ahead of print February 25, 2009.

sen reporter system is the cell surface human norepinephrine transporter (hNET), which can be imaged by single-photon emission computed tomography (SPECT) or positron emission tomography (PET) by using the radiotracer metaiodobenzylguanidine (MIBG) (10,11). The use of hNET-MIBG reporter imaging is particularly attractive from an investigative standpoint because hNET is a human protein that will not induce immune responses in humans and is expressed only in the central and peripheral sympathetic nervous systems (12). Moreover, MIBG is a standard radiopharmaceutical approved by the U.S. Food and Drug Administration. Previously, attempts to image gene-transfer therapy by PET using hNET-MIBG reporter imaging were successful in transduced cells and xenografts (11). The feasibility of imaging nonreplicating adenovirus expressing the hNET by using the hNET/¹¹C-m-hydroxyephedrine reporter gene/probe has also been demonstrated (13). In that study, however, only one of three adenovirus-transduced tumors could be visualized owing to low transduction efficiency and lack of replication. We have previously reported that the recombinant VACV GLV-1h68 does preferentially enter and replicate well within human tumors. The viral titer in colonized tumors reached as high as 1×10^9 plaque-forming units (PFUs) per gram of tissue (5). Thus, we expect that the higher expression levels of the hNET protein in tumors will result in a higher sensitivity of PET imaging. Here, we report on the construction and characterization of a novel recombinant vaccinia virus derivative of GLV-1h68, GLV-1h99, which carries the hNET expression cassette under the control of the VACV synthetic early promoter (PE). We have shown that expression of the hNET protein did not have negative effects on virus replication, cytolytic activity in cell culture, or *in vivo* virotherapeutic efficacy. GLV-1h99 efficiently eliminated tumors in mice, and the tumors infected with GLV-1h99 were readily imaged by [¹²⁴I]-MIBG PET.

MATERIALS AND METHODS

Virus and Cell Culture

African green monkey kidney fibroblast CV-1 cells and human pancreatic ductal carcinoma PANC-1 cells were purchased from American Type Culture Collection (Manassas, VA, USA) and were grown in Dulbecco's modified Eagle's medium supplemented with 1% antibiotic-antimycotic solution (Mediatech, Herndon, VA, USA) and 10% fetal bovine serum (FBS, Mediatech) at 37°C under 5% CO₂. GI-101A cells were cultured in RPMI-1640 containing 1% HEPES, 1% sodium pyruvate, 1% antibiotic-antimycotic solution, and 20% FBS. GLV-1h68 was derived from VACV L1VP, as described previously (5).

Construction of hNET Transfer Vector

hNET cDNA inserted in a pBluescript II KS+ backbone using the *Not* I and *Bam*H I sites was provided by Inna Serganova (Blasberg Laboratory at Memorial Sloan-Kettering Cancer Center, New York, NY, USA). It was PCR-amplified using pBSII-hNET as the template with primers hNET5 [5'-GTCCGAC (*Sal* I) GCCACCATGCTTCTGGCGCGGATGA A-3'] and hNET3 [5'-GATATC (*Eco*R V) TCAGATGGCCAGCCAGTGTT-3']. The PCR product was gel-purified, and cloned into the pCR-Blunt II-TOPO vector using the Zero Blunt TOPO PCR Cloning Kit (Invitrogen, Carlsbad, CA, USA). The resulting construct pCRII-hNET1 was sequence-confirmed. The hNET cDNA was released from pCRII-hNET1 with *Sal* I and *Eco*R V, and subcloned into the intermediate vector pCR-SE1, pre-cut with *Sal* I and *Sma* I. This step put hNET cDNA downstream of the sequence for PE. The viral hNET expression cassette (PE-hNET) was then released from this intermediate construct by *Bam*H I and *Hind* III and inserted into the same cut viral transfer vector pNCVf14.5T (Chen N *et al.*, unpublished data). The final construct FSE-hNET1 was sequence-confirmed and used for insertion of PE-hNET into the *F14.5L* locus in GLV-1h68.

Generation of hNET-Expressing VACV

CV-1 cells were infected with GLV-1h68 at a multiplicity of infection (MOI) of 0.1 for 1 h, then transfected by use of Fugene (Roche, Indianapolis, IN, USA) with the hNET transfer vector FSE-hNET1. Two days postinfection (dpi), infected/transfected cells were harvested and the recombinant viruses were selected and plaque purified as described previously (14). The genotype of hNET-expressing VACV GLV-1h99 was verified by PCR and sequencing. Also, the lack of expression of green fluorescent protein (GFP) was confirmed by fluorescence microscopy. Expression of β-galactosidase and β-glucuronidase was demonstrated by staining with 5-bromo-4-chloro-3-indolyl-β-D-galactopyranoside (X-gal; Stratagene, La Jolla, CA, USA) and 5-bromo-4-chloro-3-indolyl-β-D-glucuronic acid (X-GlcA; Research Product International, Mt. Prospect, IL, USA), respectively.

Protein Expression Analysis

PANC-1 cells grown in 6-well plates were mock-infected or infected with GLV-1h68 or GLV-1h99 at an MOI of 0.5. At 6, 12, 24, or 48 h postinfection (hpi), cells were harvested and lysed in RIPA buffer (10 mM Tris, pH 7.4, 150 mM NaCl, 1 mM EDTA, 0.1% SDS, 1% Triton X-100, 1% sodium deoxycholate) supplemented with proteinase inhibitor cocktail (Roche, Indianapolis, IN, USA). The cell lysates were separated on a 12% SDS-PAGE, and proteins were transferred onto a nitrocellulose transfer membrane (Whatman GmbH, Dassel, Germany). The membrane was then incubated with an anti-hNET monoclonal antibody (NET17-1; Mab Technologies, Stone Mountain, CA, USA) at a dilution of 1:500, and detected using a horseradish peroxidase-labeled secondary antibody (R1349HRP; Acris Antibodies GmbH, Hiddenhausen, Germany) at a dilution of 1:2000, followed by enhanced chemiluminescence.

Immunofluorescence Microscopy

PANC-1 cells grown in a 24-well plate were mock-infected or infected with

GLV-1h68 or GLV-1h99 at an MOI of 0.001. At 24 hpi, the cells were fixed with 3.7% paraformaldehyde, and nonpermeabilized cells were incubated with an anti-hNET monoclonal antibody (NET17-1; Mab Technologies) at a dilution of 1:500, followed by the incubation with a phycoerythrin-conjugated goat anti-mouse antibody (Abcam, Cambridge, MA, USA) at a dilution of 1:100. The pictures were taken using an Olympus 1 × 71 inverted fluorescence microscope (Olympus, Tokyo, Japan) equipped with a MicroFire True Color Firewire microscope digital charge-coupled device camera (Optronics, Goleta, CA, USA).

Viral Growth Curves

PANC-1 cells grown in 6-well plates were infected with GLV-1h68 or GLV-1h99 at an MOI of 0.01 for 1 h at 37°C. The inoculum was aspirated and the cell monolayers were washed twice with 2 mL of DPBS (Mediatech). We added 2 mL of cell culture medium containing 2% FBS into each well. Three wells of each virus were harvested at 24, 48, and 72 hpi. The harvested cells were subject to three cycles of freeze-thaw and were sonicated three times for 1 min at full power before titration. The virus was titrated in CV-1 cells in duplicates.

In vitro Cytotoxicity Assay

PANC-1 cells were plated at 2×10^4 cells per well in 96-well plates and incubated in a CO₂ incubator overnight. Cells were either mock-infected or infected with GLV-1h68 or GLV-1h99 at MOIs of 0.01 and 10. Viral cytotoxicity was assayed daily for 5 d. We then added 10 μ L of culture medium or lysis buffer (9% Triton X-100) into each of the four wells of infected cells. Lactate dehydrogenase (LDH) activity in the cell supernatant and lysate was quantified using a CytoTox 96 Non-Radioactive Cytotoxicity Assay kit (Promega, Madison, WI, USA), according to the manufacturer's instructions. Results are expressed as the percentage of surviving cells. This percentage was determined using the formula: $(\text{cell lysate} - \text{supernatant})_{\text{ix}} / (\text{cell lysate} -$

$\text{supernatant})_{\text{io}} \times 100$. In the formula, $(\text{cell lysate} - \text{supernatant})_{\text{ix}}$ and $(\text{cell lysate} - \text{supernatant})_{\text{io}}$ represent LDH activity in the cells after and before infection, respectively.

Therapy of PANC-1 Tumors in Nude Mice

All mice were cared for and maintained in accordance with animal welfare regulations under an approved protocol by the Institutional Animal Care and Use Committee of Explora Biolabs (San Diego Science Center, San Diego, CA, USA). PANC-1 xenograft tumors were developed in 6- to 8-wk-old male nude mice (NCI:Hsd:Athymic Nude-Foxn1^{nu}, Harlan) by implanting 5×10^6 PANC-1 cells subcutaneously on the right hind leg. Tumor growth was recorded once a wk in three dimensions using a digital caliper. Tumor volume was calculated as $[(\text{length} \times \text{width} \times \text{height})/2]$ and reported in cubic millimeters. Twenty-seven d after tumor cell implantation, groups of eight mice each were injected with a single intravenous dose of 5×10^6 PFUs of GLV-1h68 or GLV-1h99 in 100 μ L of PBS.

Radiopharmaceuticals

¹³¹I-labeled MIBG (¹³¹I]-MIBG) was either purchased from GE Healthcare Buchler GmbH (Braunschweig, Germany) or synthesized as described (15). [¹²⁴I]-MIBG was prepared following a procedure previously reported by Moroz and et al. (11). The radiochemical purity of the final product was > 95%, with an overall yield of > 80% and specific activity of 18.5 ± 5.2 MBq/ μ mol (0.5 ± 0.14 mCi/ μ mol). The maximum specific activities (no carrier-added synthesis) for the [¹²³I]- and [¹²⁴I]-labeled compounds were 8.9 and 1.2 TBq/ μ mol (241 and 33 Ci/ μ mol), respectively.

In vivo Imaging

All animal studies were performed in compliance with all applicable policies, procedures, and regulatory requirements of the Institutional Animal Care and Use

Committee, the Research Animal Resource Center of the Memorial Sloan-Kettering Cancer Center, and the National Institutes of Health's *Guide for the Care and Use of Laboratory Animals*. Two animals bearing two subcutaneous PANC-1 xenografts, one on each flank, measuring approximately 50 mm³, were injected with 1×10^7 PFUs of GLV-1h99 intratumorally into the right-flank tumors. Two d after infection 9.25 MBq (250 μ Ci) of [¹²⁴I]-MIBG were administered via the tail vein. Potassium iodide was used to block the uptake of radioactive iodide by the thyroid. A [¹²⁴I]-MIBG PET image was acquired over 10 min, 2 h after tracer administration. Imaging was performed using a Focus 120 microPET dedicated small-animal PET scanner (Concorde Microsystems, Knoxville, TN, USA). Data acquisition and reconstruction were performed as previously described (16). Image analysis was performed using ASIPr (Siemens Pre-clinical Solutions, Knoxville, TN, USA). Regions of interest (ROIs) were manually drawn over the tumor. Four ROIs from each tumor were averaged for comparison. The measured radioactivity was expressed as %ID/g; the mean value \pm SD was recorded.

Statistical Analysis

The significance of differences between different groups was determined using a two-tailed unpaired *t* test (Excel 2003; Microsoft, Redmond, WA, USA). *P* < 0.05 was considered significant.

All supplementary materials are available online at www.molmed.org.

RESULTS

Construction of the Recombinant VACV Expressing hNET, GLV-1h99

The construct of GLV-1h99 used in this study was derived from GLV-1h68 by replacing the *Renilla* luciferase-GFP (*RUC-GFP*) expression cassette at the *F14.5L* locus with the hNET expression cassette by homologous recombination in infected cells. In GLV-1h99, hNET expression is under the control of the VACV PE. The

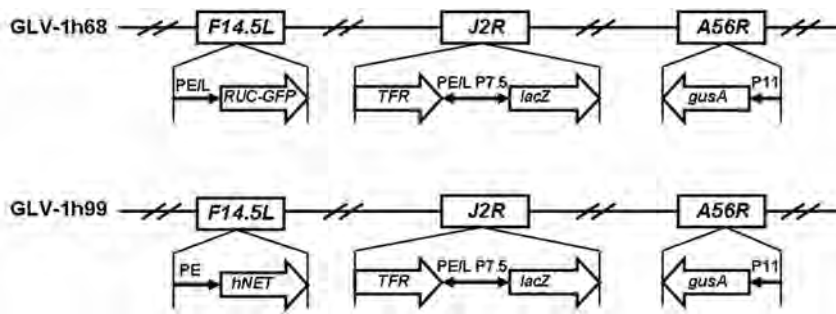


Figure 1. Schematic representation of the genomic structure of the novel recombinant VACV GLV-1h99. GLV-1h99 was derived from GLV-1h68 by replacing the *RUC-GFP* expression cassette at the *F14.5L* locus with the hNET expression cassette through *in vivo* homologous recombination. Both viruses contain *lacZ* and *gusA* expression cassettes at *J2R* and *A56R* loci, respectively. PE, PE/L, P11, and P7.5 are VACV synthetic early, synthetic early/late, 11-K, and 7.5-K promoters, respectively. *TFR* is human transferrin receptor inserted in the reverse orientation with respect to the promoter PE/L.

genotype of GLV-1h99 (Figure 1) was verified by PCR and sequencing. Lack of GFP expression was confirmed by fluorescence microscopy, and expression of β -galactosidase and β -glucuronidase was demonstrated by X-gal and X-GLcA staining, respectively (Supplementary Figure 1 online).

hNET Protein Expression Detected by Western Blot

To show hNET protein expression by GLV-1h99, PANC-1 cells were mock-infected or infected with GLV-1h99 or its parent virus GLV-1h68, and harvested at 6, 12, 24, and 48 hpi. The hNET protein was detected by Western blot analysis using monoclonal anti-hNET antibody. As shown in Figure 2, only GLV-1h99-infected cells expressed the hNET protein with increasing concentration of the protein during the first 24 hpi and slightly decreased hNET expression at 48 hpi compared with the maximum at 24 hpi. Cells either mock-infected or infected with GLV-1h68 did not express the hNET protein. Two major bands (approximately 35 and 47 kDa) were detected in GLV-1h99-infected cells. The band of 47 kDa was similar to the reported unglycosylated form of the hNET protein (17). The 35-kDa band might be a degradation product. The hNET protein was also detected in CV-1 cells infected with GLV-1h99 (data not shown).

hNET Protein Present on the Cell Surface

The hNET protein belongs to a family of Na^+/Cl^- -dependent transporters that contain multiple transmembrane domains. To determine whether the hNET protein expressed by GLV-1h99 was correctly presented on the cell membrane, we infected PANC-1 cells with GLV-1h99 and fixed them with 3.7% paraformaldehyde without cell permeabilization. The



Figure 2. Western blot analysis of the hNET protein expression in PANC-1 cells infected with GLV-1h99. PANC-1 cells were either mock-infected or infected with GLV-1h68 or GLV-1h99 at an MOI of 0.5 for 6, 12, 24, and 48 h, respectively. The hNET protein was detected by Western blot analysis using monoclonal anti-hNET antibody. Only GLV-1h99-infected cells expressed the hNET protein, but cells either mock-infected or infected with GLV-1h68 did not. The arrows indicate the different forms of the hNET protein detected in GLV-1h99-infected cells. The molecular weight marker bands (in kDa) are shown on the left.

hNET protein was visualized using the monoclonal anti-hNET antibody NET17-1 that recognizes the extracellular domain of the protein. As shown in Figure 3, mock or GLV-1h68-infected cells (as demonstrated by GFP expression) did not show hNET protein expression, whereas the hNET protein on the cell surface of PANC-1 cells infected with GLV-1h99 was readily detectable by immunofluorescence microscopy.

Expression of the hNET Protein under the Control of the PE Did Not Have Negative Effects on Virus Growth *in vitro*

Whether hNET protein expression would affect VACV replication was unknown. To evaluate the effect of hNET protein expression on VACV replication, PANC-1 cells were infected with either GLV-1h99 or its parent virus, GLV-1h68, at an MOI of 0.01, and the infected cells were harvested at 24, 48, and 72 hpi. The viral titers at each time point were determined in CV-1 cells using standard plaque assays. GLV-1h99 gave significantly higher viral yields ($P < 0.01$) at all time points in comparison with its parent virus, GLV-1h68 (Figure 4), indicating that expression of the hNET protein under the control of the PE did not have negative effects on virus growth *in vitro*. This experiment was repeated once and similar results were obtained.

Expression of the hNET Protein Did Not Affect Cytolytic Activity of VACV in Cell Cultures

To investigate whether expression of hNET would affect cytolytic activity of VACV in cell cultures, PANC-1 cells were infected with GLV-1h68 or GLV-1h99 at both low (0.01) and high (10) MOIs. Viral cytotoxicity was measured daily for 5 d. At the MOI of 10, initially most of the tumor cells were infected. The survival curves for GLV-1h68 and GLV-1h99 were almost identical, indicating that the cells infected by either of the virus strains were dying at similar levels. The infected cells started to die on the second day of infection. By d 4, about 70% of the tumor

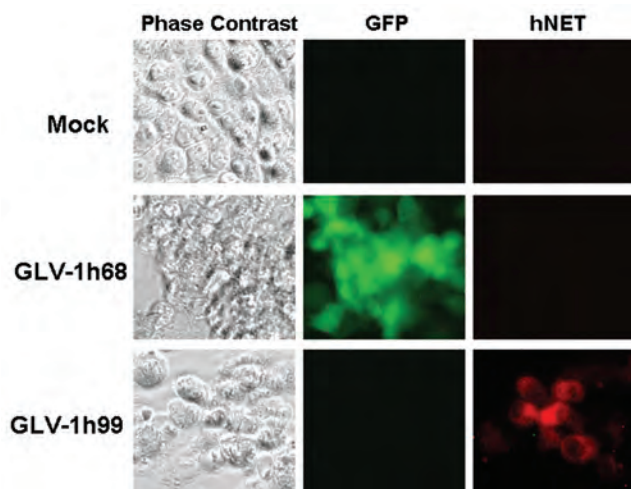


Figure 3. Localization of the hNET protein on the cell membrane of nonpermeabilized PANC-1 cells infected with GLV-1h99. PANC-1 cells were mock-infected or infected with GLV-1h68 or GLV-1h99 at an MOI of 0.001 for 24 h. The hNET protein was detected by immunofluorescence microscopy using monoclonal anti-hNET antibody NET17-1, which recognizes the extracellular domain of the protein. Mock- or GLV-1h68-infected cells (as demonstrated by GFP expression) did not express the hNET protein, whereas the hNET protein on the cell membrane of PANC-1 cells infected with GLV-1h99 was readily detectable.

cells were killed by both virus strains (Figure 5). However, at the MOI of 0.01, initially only a small portion of cells was infected. The cells in infected wells continued to grow within 2 d of infection, and thereafter cell numbers started to decline on d 3 postinfection. By d 5, more

than 90% of the cells were killed by GLV-1h68 as well as by GLV-1h99. Although survival curves for GLV-1h68 and GLV-1h99 were similar, the percentages of cell survival after GLV-1h99 infection were consistently lower than after GLV-1h68 infection at all time points except for 72

hpi. The difference in percentages of cell survival after GLV-1h99 and GLV-1h68 infection was statistically significant ($P < 0.001$) at 96 hpi, indicating that GLV-1h99 showed slightly better cytolytic activity. This finding is consistent with the enhanced replication of GLV-1h99 in PANC-1 cells, as shown earlier. It is important to note that the growth pattern of infected tumor cells in tissue culture mimicked the infected tumor growth pattern in mice. This experiment was repeated once and similar results were obtained.

Expression of the hNET Protein Did Not Have a Negative Effect on Vaccinia Virotherapy

Previously, we showed that GLV-1h68 was able to eradicate solid human breast and pancreatic tumors in nude mice after a single intravenous application (5,18). To find out whether replacing the *RUC-GFP* expression cassette in GLV-1h68 with the hNET expression cassette would negatively affect viral-therapeutic effects, we treated human pancreatic tumors in nude mice with either GLV-1h68 or GLV-1h99. The growth of tumors treated with GLV-1h68 occurred in three distinct phases: growth, inhibition, and regression, as described previously (5). The tumors treated with GLV-1h99 showed a similar growth pattern, but tumor shrinkage was observed 1 wk earlier than with GLV-1h68-treated tumors (Figure 6). The size of tumors treated with GLV-1h99 was significantly smaller than that treated with GLV-1h68 on d 21 after virus administration and thereafter ($P < 0.05$). Obviously, expression of the hNET protein did not seem to have a negative effect on vaccinia virotherapy. The accelerated tumor shrinkage by GLV-1h99 was predicted by the enhanced viral replication and cytotoxicity in tissue culture in comparison with its parental virus, GLV-1h68. This experiment was repeated once and similar results were obtained. GLV-1h99 also showed better therapeutic efficacy than GLV-1h68 when human breast GI-101A tumors in nude mice were treated (data not shown).

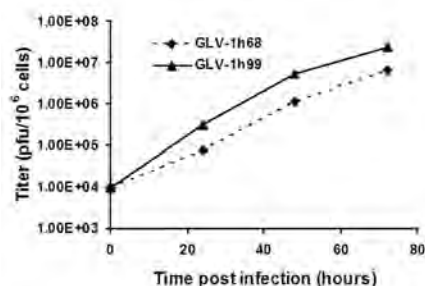


Figure 4. GLV-1h99 growth curve in PANC-1 cells. PANC-1 cells grown in 6-well plates were infected with GLV-1h68 or GLV-1h99 at an MOI of 0.01. Three wells of each virus were harvested at 24, 48, and 72 hpi. GLV-1h99 gave significantly higher viral yields ($P < 0.01$) at all time points compared with its parent virus, GLV-1h68. The values are the mean of triplicate samples, and the bars indicate SD. Representative of two independent experiments.

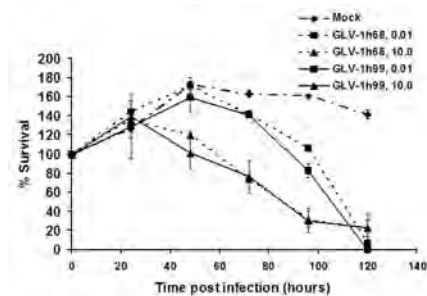


Figure 5. Tumor cell killing in cell cultures by GLV-1h99. PANC-1 cells were infected with GLV-1h68 or GLV-1h99 at MOIs of 0.01 and 10. Cell viability was determined using CytoTox 96 Non-Radioactive Cytotoxicity Assay kit (Promega, Madison, WI, USA). Cell viability before infection was set at 100%. The values are the mean of quadruple samples, and the bars indicate SD. Representative of two independent experiments.

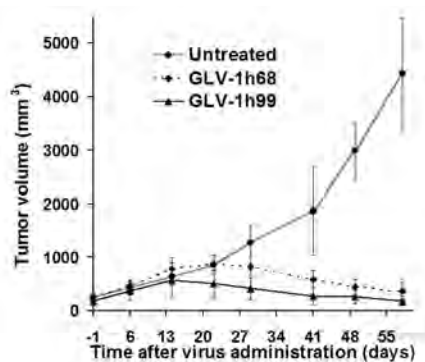


Figure 6. Therapy of human pancreatic ductal carcinoma PANC-1 in nude mice with GLV-1h99. Both GLV-1h68 and GLV-1h99 can shrink PANC-1 tumors. The tumors treated with GLV-1h99 started to shrink 1 wk earlier than GLV-1h68-treated tumors. The values are the mean of eight samples, and the bars indicate SD. Representative of two independent experiments.

In vivo Imaging of Tumors Infected with GLV-1h99

Next we investigated whether the GLV-1h99-mediated expression of the hNET protein resulted in specific uptake of the radiotracer [¹³¹I]-MIBG. This radiotracer can be used for noninvasive imaging of functional norepinephrine transporter (19). Preliminary studies were performed to confirm that [¹³¹I]-MIBG accumulated in GLV-1h99-infected GI-101A and PANC-1 cells *in vitro* (results not shown). GLV-1h68 mock-infected PANC-1 cells retained only minimal amounts of the radiotracer. Therefore, GLV-1h99 led to expression of a functional norepinephrine transporter, which resulted in the specific uptake of [¹³¹I]-MIBG.

After successful cell culture uptake studies, we wanted to show the feasibility of using GLV-1h99 in combination with MIBG to image infected PANC-1 tumors. Therefore, hNET protein expression in the PANC-1 tumor-bearing animals after GLV-1h99 administration was visualized by [¹²⁴I]-MIBG PET. [¹²⁴I]-MIBG was intravenously administered 48 h after intratumoral virus injection, and PET imaging was performed 2 h

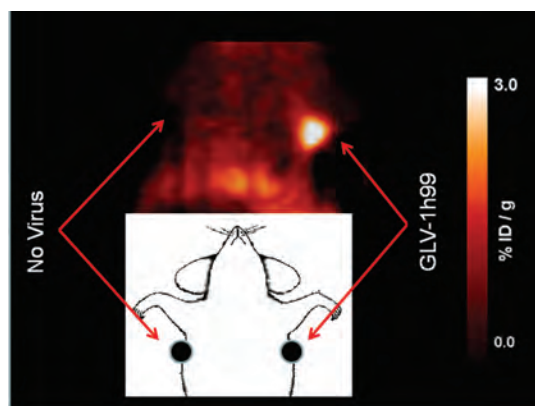


Figure 7. [¹²⁴I]-MIBG PET scan 48 h after infection. We injected, respectively, 1×10^7 PFUs of GLV-1h99 and PBS intratumorally into the right flank tumor ($\sim 50 \text{ mm}^3$) of the mouse bearing PANC-1 tumors on both sides. The scan was obtained 2 h after systemic radiotracer administration.

after radiotracer administration. Tumor radioactivity values (%ID/g) were measured. The levels of radioactivity in the PANC-1 tumors after injection of GLV-1h99 were 1.56 ± 0.64 and 1.74 ± 0.61 , compared with 0.88 ± 0.10 and 0.83 ± 0.11 in tumors that were injected with PBS 48 h prior to [¹²⁴I]-MIBG administration. The values from PBS-injected tumors were hardly above the background uptake that made the tumors hardly visible whereas the GLV-1h99-injected tumors were readily detectable (Figure 7). Usually radioactivity of 1.5 \times to 2 \times above the background is easily detected by PET scanning. A GLV-1h68 control was not included in this experiment because the *in vitro* radiotracer uptake experiment showed that PANC-1 cells infected with GLV-1h68 did not significantly take up the radiotracer, and nearly the same low tumor-to-organ radioactivity ratios were found for the GLV-1h68 and PBS control groups of animals (data not shown). In another experiment, 5 athymic *nu/nu* female mice with orthotopic pleural mesothelioma were injected with 1×10^7 PFUs of GLV-1h99 intrapleurally. The viral localization was successfully visualized by [¹²⁴I]-MIBG PET imaging of the hNET protein expression in tumors both at 48 and 72 hpi, although the highest levels of radioactivity in the tumors were found 48 hpi. The only low levels

of radioactivity were observed in the tumors injected with GLV-1h68 or PBS (data not shown). The presence of the virus in tumors was confirmed by immunohistochemistry staining of tumors using X-gal for *lacZ* expression (data not shown).

DISCUSSION

VACV is arguably the most successful biologic therapy agent, because versions of this virus were given to millions of humans during the smallpox eradication campaign (20). Recently, attention has focused on using this family of viruses in the treatment of cancer, either as cancer vaccines or as oncolytic virotherapeutic agents. Various recombinant versions of this virus have been used to lyse tumor cells *ex vivo* and *in vivo* to stimulate the native immune response to cancer (21,22). More recently, engineered VACVs have also been successfully used as direct oncolytic agents, capable of preferentially infecting, replicating within, and killing a wide variety of cancer cell types (23–25). One such promising virus is GLV-1h68. This virus has shown efficacy in the treatment of malignant pleural mesothelioma, breast cancer, anaplastic thyroid cancer, and pancreatic cancer (5,18,23,26), and is currently being tested in phase I human trials. In this report we describe experiments that led to the gen-

eration of a novel recombinant VACV derived from GLV-1h68, GLV-1h99, with the additional capability of facilitating noninvasive imaging of tumors and metastases. To our knowledge, GLV-1h99 is the first oncolytic virus expressing the hNET protein that can efficiently eliminate tumors and simultaneously facilitate deep-tissue imaging of infected tumors. We believe that the GLV-1h99 virus is a promising candidate for future clinical studies combining deep-tissue imaging and oncolytic virotherapy.

VACV gene transcription occurs in a temporal manner, with early genes transcribed within the core of the virus particle soon after infection, whereas intermediate and late genes transcribe in the cytoplasm of infected cells after viral DNA replication. The early, intermediate, and late mRNA synthesis was detectable within 20, 100, and 140 minutes of infection, respectively (27). The strength of vaccinia promoters also varies. The vaccinia promoters PE, synthetic early/late (PE/L), and synthetic late (PL) are very well studied. PE is the weakest among the three promoters, but is stronger than native early promoters, whereas PE/L is comparable to or slightly stronger than PL. Initially, we tried to generate recombinant VACVs expressing the hNET protein under the control of all three promoters (PE, PE/L, and PL) to evaluate the effect of the levels and temporal manner of hNET protein expression on virus replication, therapy, and imaging. The use of a PE/L or PL at the *F14.5L* locus failed to generate any recombinants. Overexpression and/or constitutive expression of hNET seemed to be toxic to the virus. We were able to generate, however, a recombinant virus that expressed the hNET protein under the control of the PE. Western blot studies showed that the hNET protein expression in PANC-1 cells infected with GLV-1h99 at an MOI of 0.5 became detectable at 6 hpi and reached the maximum at 24 hpi, followed by a slight decline at 48 hpi. The lower level of the protein detected at 48 hpi was probably due to cell killing by the virus. The hNET protein

was properly transported to the cell membrane, as demonstrated by fluorescence microscopy.

The hNET protein belongs to a family of Na⁺/Cl⁻-dependent transporters that contain multiple transmembrane domains, mediating the transport of norepinephrine, dopamine, and epinephrine across the cell membrane. GLV-1h99-mediated expression of the hNET protein in both infected PANC-1 and GI-101A cells resulted in specific uptake of the radiotracer [¹³¹I]-MIBG, indicating that the functional hNET protein was expressed on the cell membrane of GLV-1h99-infected cells. In PANC-1 cells, the uptake of [¹³¹I]-MIBG reached the maximum at 24 hpi and started to decrease at 48 hpi, correlating well with the hNET protein expression level observed in the Western blot studies (data not shown). In mice, two PANC-1 tumors infected with GLV-1h99 were readily detectable by PET. In a separate experiment, five GLV-1h99-infected orthotopic pleural mesothelioma tumors were also successfully imaged by [¹²⁴I]-MIBG PET. In contrast, only 1 of 3 tumors transduced by the hNET expressing nonreplicating adenovirus was reported to be visible by PET (13). The better performance by GLV-1h99 could be attributable to its higher infection efficiency and replication and spreading capabilities. To our knowledge, GLV-1h99 is the first oncolytic virus that expresses hNET.

The most important characteristic of an oncolytic agent, however, is its ability to infect, replicate within, and kill tumor cells. The exploitation of the natural life cycle of viruses is the basis of the entire field of oncolytic virotherapy. VACV has many characteristics desirable in an oncolytic virus: (a) It has a short, well-characterized life cycle and spreads very rapidly from cell to cell; (b) it is highly cytolytic for a broad range of tumor cell types; (c) it has a large insertion capacity (>25 kb) for the expression of exogenous genes; (d) it is genetically very stable; (e) it enables large-scale production of high levels of infectious viruses; (f) it does not cause any known diseases in humans;

(g) it does not integrate into the host genome; and (h) it was used as smallpox vaccine in millions of people and thus has well-documented side effects. These features make VACV an excellent choice as a therapeutic agent for cancer virotherapy. Other viruses, including adenoviruses, herpes simplex viruses, and Newcastle disease viruses, underwent or are presently undergoing clinical testing for cancer therapy in humans. The novel VACV GLV-1h99 was effective at killing cancer cells and eradicating tumors in cell culture and in a xenograft model, respectively. These results indicated that expression of the hNET protein did not negatively affect virus replication, cytolytic activity in cell culture, or *in vivo* virotherapeutic efficacy. In fact, viral replication and oncolytic effects seem to be slightly improved owing to the exchange of expression cassettes. These enhanced effects could not be due to the function of the hNET protein. Instead, the difference in promoter strength between the PE that drives hNET expression and the PE/L that controls the substituted *RUC-GFP* expression in GLV-1h68 might explain the difference in viral replication. PE/L was shown to be more than 100 times stronger than PE (28). We also found that virus replication in cell culture was inversely proportionate to the strength of promoters used in foreign gene expression inserted into the viral genome (data not shown).

The tumor system in the investigation we reported here was pancreatic adenocarcinoma. This is an aggressive cancer that is almost uniformly fatal, with a median survival of 6–12 months (29). Furthermore, most pancreatic adenocarcinomas are resistant to chemotherapy and to radiation therapy. Thus, the significant efficacy that GLV-1h99 showed against pancreatic tumors justifies further studies, as well as the initiation of clinical trials. These encouraging results should not only stimulate future studies of the use of MIBG-scanning in the monitoring of GLV-1h99 therapy, but also suggest its dual function in general as a therapy for pancreatic cancer.

ACKNOWLEDGMENTS

We thank Terry Trevino, Johanna Langbein, and Rosana Magpantay for excellent technical support, and Andrea Feathers for editorial support. This work was supported by grants from Genelux Corporation (R&D facility in San Diego, CA, USA). The hNET plasmid construction and imaging was supported by NIH grants R25T-CA096945, P50 CA86438, and DOE grant FG03-86ER60407. Services provided by the MSKCC Small-Animal Imaging Core Facility, supported in part by NIH Small-Animal Imaging Research Program (SAIRP) Grant No R24 CA83084 and NIH Center Grant No P30 CA08748, are gratefully acknowledged. Y Fong was partly supported by a grant from the Flight Attendant's Medical Research Institute.

DISCLOSURES

N Chen, Q Zhang, YA Yu, J Stritzker, and AA Szalay are employees of Genelux Corporation. No competing financial interests exist for P Brader, A Schirbel, S Samnick, I Serganova, R Blasberg, and Y Fong.

REFERENCES

- Vasey PA, et al. (2002) Phase I trial of intraperitoneal injection of the E1B-55-kd-gene-deleted adenovirus ONYX-015 (dl1520) given on days 1 through 5 every 3 weeks in patients with recurrent/refractory epithelial ovarian cancer. *J. Clin. Oncol.* 20:1562-9.
- Adusumilli PS, et al. (2006) Real-time diagnostic imaging of tumors and metastases by use of a replication-competent herpes vector to facilitate minimally invasive oncological surgery. *FASEB J.* 20:726-8.
- Sinkovics JG, Horvath JC. (2000) Newcastle disease virus (NDV): brief history of its oncolytic strains. *J. Clin. Virol.* 16:1-15.
- Woo Y, et al. (2008) Myxoma virus is oncolytic for human pancreatic adenocarcinoma cells. *Ann. Surg. Oncol.* 15:2329-35.
- Zhang Q, et al. (2007) Eradication of solid human breast tumors in nude mice with an intravenously injected light-emitting oncolytic vaccinia virus. *Cancer Res.* 67:10038-46.
- Barber GN. (2004) Vesicular stomatitis virus as an oncolytic vector. *Viral Immunol.* 17:516-27.
- Adusumilli PS, et al. (2007) Radiation-induced cellular DNA damage repair response enhances viral gene therapy efficacy in the treatment of malignant pleural mesothelioma. *Ann. Surg. Oncol.* 14:258-69.
- Petrowsky H, et al. (2001) Functional interaction between fluorodeoxyuridine-induced cellular alterations and replication of a ribonucleotide reductase-negative herpes simplex virus. *J. Virol.* 75:7050-8.
- Roizman B, Joklik W, Fields B, Moss B. (1994) The destruction of smallpox virus stocks in national repositories: a grave mistake and a bad precedent. *Infect. Agents Dis.* 3:215-7.
- Shulkin BL, et al. (1986) Iodine-123-4-amino-3-iodobenzylguanidine, a new sympathoadrenal imaging agent: comparison with iodine-123 meta-iodobenzylguanidine. *J. Nucl. Med.* 27:1138-42.
- Moroz MA, et al. (2007) Imaging hNET reporter gene expression with 124I-MIBG. *J. Nucl. Med.* 48:827-36.
- Axelrod J, Kopin IJ. (1969) The uptake, storage, release and metabolism of noradrenaline in sympathetic nerves. *Prog. Brain Res.* 31:21-32.
- Buursma AR, et al. (2005) The human norepinephrine transporter in combination with 11C-m-hydroxyephedrine as a reporter gene/reporter probe for PET of gene therapy. *J. Nucl. Med.* 46:2068-75.
- Falkner FG, Moss B. (1990) Transient dominant selection of recombinant vaccinia viruses. *J. Virol.* 64:3108-11.
- Samnick S, Kirsch CM. (1999) A simple and rapid routine preparation of no-carrier added meta-I-123- and I-131-iodobenzylguanidine (I-123-MIBG and I-131-MIBG) for clinical nuclear medicine applications [in German]. *Nuklearmedizin* 38:292-6.
- Brader P, et al. (2008) Escherichia coli Nissle 1917 facilitates tumor detection by positron emission tomography and optical imaging. *Clin. Cancer Res.* 14:2295-302.
- Melikian HE, et al. (1994) Human norepinephrine transporter: biosynthetic studies using a site-directed polyclonal antibody. *J. Biol. Chem.* 269:12290-7.
- Yu YA, et al. (2009) Regression of human pancreatic tumor xenografts in mice after a single systemic injection of recombinant vaccinia virus GLV-1h68. *Mol. Cancer Ther.* 8:141-51.
- Anton M, et al. (2004) Use of the norepinephrine transporter as a reporter gene for non-invasive imaging of genetically modified cells. *J. Gene Med.* 6:119-26.
- Thorne SH, Hwang TH, Kirn DH. (2005) Vaccinia virus and oncolytic virotherapy of cancer. *Curr. Opin. Mol. Ther.* 7:359-65.
- Pantuck AJ, et al. (2004) Phase I trial of antigen-specific gene therapy using a recombinant vaccinia virus encoding MUC-1 and IL-2 in MUC-1-positive patients with advanced prostate cancer. *J. Immunother.* 27:240-53.
- Marshall JL, et al. (2005) Phase I study of sequential vaccinations with fowlpox-CEA(6D)-TRICOM alone and sequentially with vaccinia-CEA(6D)-TRICOM, with and without granulocyte-macrophage colony-stimulating factor, in patients with carcinoembryonic antigen-expressing carcinomas. *J. Clin. Oncol.* 23:720-31.
- Lin SF, et al. (2007) Treatment of anaplastic thyroid carcinoma in vitro with a mutant vaccinia virus. *Surgery* 142:976-83.
- Chalikonda S, et al. (2008) Oncolytic virotherapy for ovarian carcinomatosis using a replication-selective vaccinia virus armed with a yeast cytosine deaminase gene. *Cancer Gene Ther.* 15:115-25.
- Chang E, et al. (2005) Targeting vaccinia to solid tumors with local hyperthermia. *Hum. Gene Ther.* 16:435-44.
- Kelly KJ, et al. (2008) Novel oncolytic agent GLV-1h68 is effective against malignant pleural mesothelioma. *Hum. Gene Ther.* 19:774-82.
- Baldick CJ Jr, Moss B. (1993) Characterization and temporal regulation of mRNAs encoded by vaccinia virus intermediate-stage genes. *J. Virol.* 67:3515-27.
- Chakrabarti S, Sisler JR, Moss B. (1997) Compact, synthetic, vaccinia virus early/late promoter for protein expression. *Biotechniques* 23:1094-7.
- Ferrone CR, et al. (2008) Pancreatic adenocarcinoma: the actual 5-year survivors. *J. Gastrointest. Surg.* 12:701-6.